

Optical properties of Er³⁺ doped phosphate glasses

Mahmoud Mohammed Ismail*,¹ Hazem Farouk,² Mohamed Ali Salem,¹ Adel Ashery,¹
Inas Kamal Battisha¹

¹ National Research Centre, Solid State Physics Department, Physics Research Division, 33 El Behooth St., Dokki, Giza, Egypt, (Affiliation ID: 60014618).

² Al AZHAR University, Physics department, faculty of science, Cairo, Egypt.

Abstract:

Er³⁺-doped Na-Al-Ba-K phosphate glasses were prepared by melt quenching technique. The absorbance spectrum was measured and hence the absorption coefficient, absorption cross-section were calculated. The emission cross-section has been evaluated using Mc-Cumber theory. The gain has been evaluated as a function of population inversion which show that the amplification action would be achieved around 1596 nm for a population inversion of only 20%. The Judd-Ofelt analysis has been carried out and hence the radiative properties of $^4I_{13/2} \rightarrow ^4I_{15/2}$ and $^4S_{3/2} \rightarrow ^4I_{15/2}$ transitions were obtained. Higher radiative lifetime for the $^4I_{13/2}$ level of Er³⁺ ion has been noticed compared to the other Er³⁺ doped glasses. These results clearly indicate that the present glasses are suitable for laser as well as optical amplifiers around 543 nm and 1522nm.

Keywords :- Phosphate glass, Erbium, Judd-Ofelt, Mc-Cumber, Optical properties

1 Introduction

In recent years, great efforts dedicated to study the optical properties of trivalent erbium (Er³⁺) ions -doped different glasses for the development of optical devices such as solid state lasers, optical sensors and optical amplifiers, etc. Er³⁺ ion exhibits prominent emissions around 1522 nm corresponding to $^4I_{13/2} \rightarrow ^4I_{15/2}$ transition. This transition attracted attention since it is located in the so-called ultra low-loss telecommunication window of glass, extending from around 1450 to 1600 nm and it is also located in the eye-safe spectral region [M. Yamada 1997, Y. Ohishi 1998]. In addition, Er³⁺ ion emits green emission around 540 nm corresponds to $^4S_{3/2} \rightarrow ^4I_{15/2}$ transition which could be useful for green laser applications [A. Lira 2004].

The optical properties of rare earth (R.E) ions depend on their local environment in which they are incorporated. In other words, the surrounding ligand field has a considerable influence on the optical properties of the R.E ion such as the absorption and emission cross-section, spectral shapes of the emission and absorption bands as well as excited state lifetimes, which are the key factors in amplification and lasing processes.

*Corresponding author : mah_m1985@yahoo.com

Other than optical properties, the host materials should have good thermal, mechanical and chemical stability to be suitable for high performance optical devices. The phosphate based multi-component glasses have received enormous interest because of high R.E ions solubility without clustering, low non-linear refractive index [M.Yamane and Y.Asahara 2004] and the phonon energy of phosphate glasses ($\sim 1200 \text{ cm}^{-1}$), makes it almost insensitive to up-conversion phenomena [Digonett 2001].

The main purpose of this work is dedicated to prepare multi-component phosphate glasses doped with Er^{3+} ions. The structure, composition, physical and optical properties of the prepared sample will be evaluated.

2 Experimental details

2.1 Glass preparation

Phosphate glasses with the composition (mol%) of $60\% \text{ P}_2\text{O}_5 + 8\% \text{ Al}_2\text{O}_3 + 2\% \text{ Na}_2\text{O} + 13\% \text{ BaO} + (17-x)\% \text{ K}_2\text{O} + x\% \text{ Er}_2\text{O}_3$ ($x = 0.2, 0.75, \text{ and } 1.5 \%$) were prepared using conventional melt quenching technique which symbolic as PANBK0.2Er, PANBK0.75Er, and PANBK1.5Er.

High purity P_2O_5 , Al_2O_3 , Na_2CO_3 , BaCO_3 , K_2CO_3 , and $\text{Er}(\text{NO}_3)_3 \cdot 5\text{H}_2\text{O}$ were used as starting materials to prepare the glasses. A batch of 30 grams of starting materials was thoroughly mixed in agate mortar and the homogeneous mixture was taken in a Porcelain crucible and kept in an electric furnace at a temperature of 1100°C for 2 h. The melt was then poured onto a preheated stainless steel mold at a temperature of 430°C until the glass solidifies. Then the glass samples were annealed at the same temperature 430°C for 10 hours to remove thermal strains and stress. After that the samples were allowed to cool to room temperature. Finally, the prepared glasses were cut and polished for optical measurements.

2.2 Characterization techniques

The density of the samples was determined by Archimede's method with water as an immersion liquid. The refractive indices of this glasses were measured using PTR 46X refractometer at 589 nm with the monobromonaphthalene as the contact layer between the Samples and prism of the refractometer. X-ray diffraction (XRD) patterns for the prepared samples were recorded with a Philips X-ray diffractometer using monochromatized $\text{CuK}_{\alpha 1}$ radiation of wavelength 1.54056 \AA from a fixed source operated at 45 kV and 9 mA. SEM model QUANTA -FEG250 and operating at 35 kV employed in the present work to study coarse and fine microstructures of the samples. Attached Energy dispersive X-ray (EDX) unit were used to study the atomic ratios of the elements for samples. Absorption spectra (200-1800 nm) were measured using a UV/VIS/NIR spectrophotometer Model V-570. The instrument specified by resolution 0.1 nm and wavelength accuracy $\pm 0.3 \text{ nm}$ (at a spectral bandwidth of 0.5 nm). The measurements were made on glasses and glasses powder, immediately after glass preparation and all spectra were measured at room temperature

3 Results and discussion

3.1 Physical properties

The density of the samples was determined by Archimede's method with water as an immersion liquid using the following relation

$$\rho = \frac{W_a}{W_a - W_w} \rho_w \quad (1)$$

Where W_a is the weight in air, W_w is the weight in water, ρ is the glass density and ρ_w is the density of water.

The average molecular weight of a given sample (M_w) which composed of many elements is given by the following relation

$$M_w = \sum r_i m_i \quad (2)$$

Where m_i is the atomic mass of the element and r_i is the ratio of that element

The Er^{3+} ions concentration (N) is obtained using the following relation [Reddy 2011].

$$N \text{ (ions/cm}^3\text{)} = \frac{2 N_a \rho x}{M_w} \quad (3)$$

where x is the molar ratio of Er^{3+} ions and N_a is Avogadro's number.

Table 1 shows the density, ions concentration and average molecular weight of PANBK0.2Er, PANBK0.75Er and PANBK1.5Er glasses. It can be noticed that M_w , and ρ slightly increase with the increase in Er content and this is due to that Er atom is much heavier than K atom.

Table 1. The physical properties of PANBK0.2Er, PANBK0.75Er and PANBK1.5Er glasses.

| Samples | Physical properties | | |
|-------------|------------------------|--|------------------|
| | $\rho(\text{gm/cm}^3)$ | $N(\times 10^{+20} \text{ ions/cm}^3)$ | $M_w(\text{gm})$ |
| PANBK0.2Er | 2.79 | 0.5123 | 131.08 |
| PANBK0.75Er | 2.80 | 1.9044 | 132.67 |
| PANBK1.5Er | 2.82 | 3.77313 | 134.83 |

3.2 XRD

Fig .1 shows the XRD patterns of the samples doped with different concentrations of Er^{3+} . Very broad hump extending from $2\Theta = 12$ up to 40° is observed. No diffraction patterns were noticed all over the measured range for all of the samples which confirm the amorphous nature of our glasses.

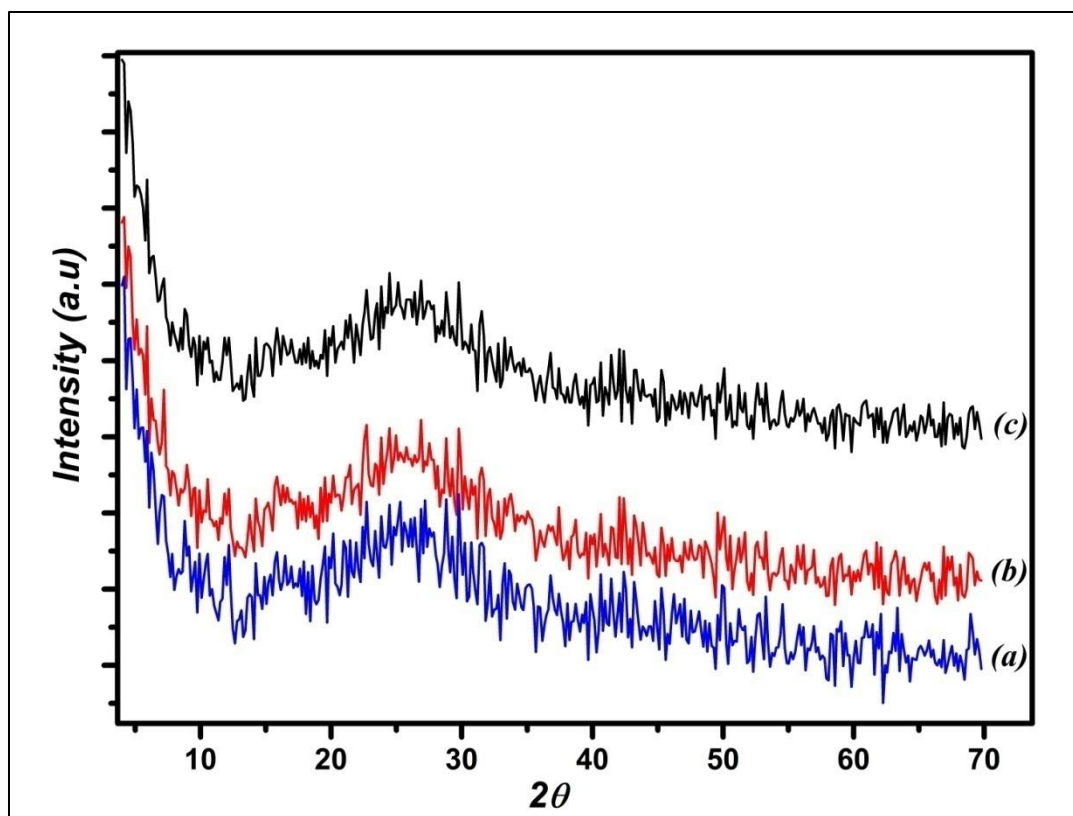


Fig.1. The XRD patterns of PANBK0.2Er (a), PANBK0.75Er (b) and PANBK1.5Er (c).

3.3 SEM.

Fig.2 shows the SEM images of the PANBK0.2Er as a representative sample. The SEM images show the surface morphology of the samples. The appeared smooth surfaces confirm the dense nature presence of the glass matrix. We couldn't identify any grain boundaries from the surface morphological image which confirms the amorphous nature of the samples. The obtained data coincides with XRD spectra.

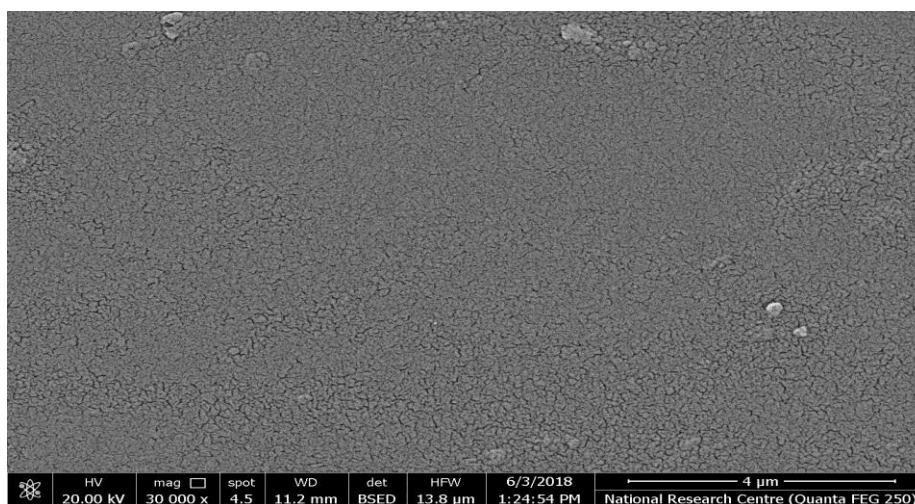


Fig.2. The FESEM images of the PANBK0.2Er sample.

3.4 EDX

Fig.3 shows the EDAX spectra of the PANBK0.2Er glass sample. The EDX spectra confirm the existence of Phosphate, Aluminum, Sodium, Potassium, Barium and Erbium in the glass matrix.

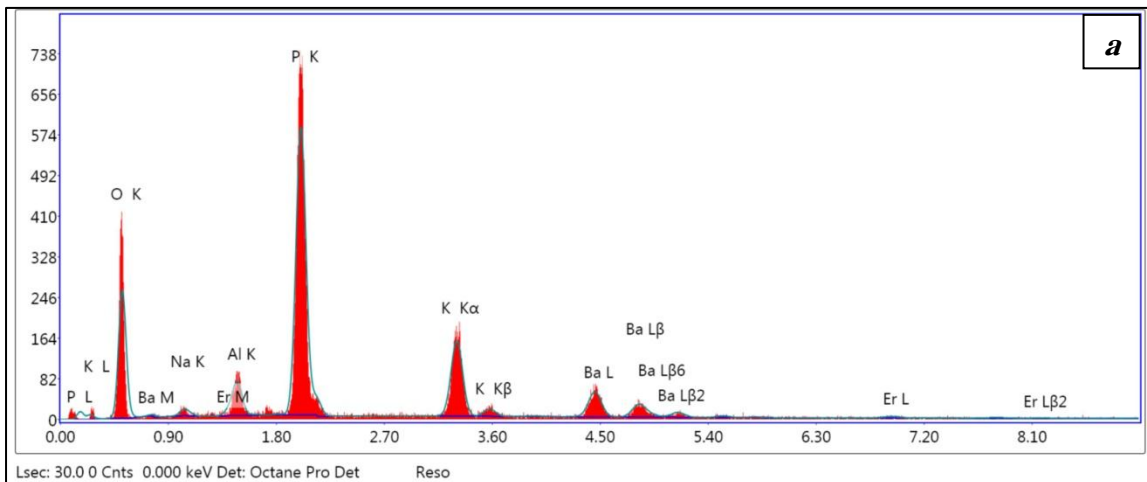


Fig.3. The EDX spectra of the PANBK0.2Er.

Table 2 shows the atomic ratios of the elements and the oxygen to phosphate ratio for PANBK0.2Er glass, they are equal to 2.985 % and 2.994, respectively, which indicate that the glasses are almost a meta-phosphate glasses.

Table 2. The atomic ratios of elements and oxygen to phosphate ratio for PANBK1.0Er and PANBK0.5Er glasses.

| Sample | P | Al | Na | K | Ba | Er | O | O/P ratio |
|------------|-------|--------|-------|-------|------|------|--------|-----------|
| PANBK0.2Er | 21.5% | 2.68 % | 1.25% | 6.8 % | 2.7% | 0.2% | 64.84% | 3.016 % |

3.5 Optical properties

Fig.4 shows absorption Coefficient spectra of PANBK1.5Er glass as a representative data in the region extended from 300 up to 1650 nm. The spectrum consists of 11 bands corresponding to the transitions from the ground state $^4I_{15/2}$ to the various excited states $^4I_{13/2}$, $^4I_{11/2}$, $^4I_{9/2}$, $^4F_{9/2}$, $^4S_{3/2}$, $^2H_{11/2}$, $^4F_{7/2}$, $^4F_{5/2}$, $^2G_{9/2}$, $^4G_{11/2}$ and $^4G_{9/2}+^2K_{15/2}$, respectively. The absorption bands are assigned to the energy levels of reported Er⁺³ glass systems [Babu 2007, C.C.Santos 2009, Reddy 2011, Luewarasirikul 2018].

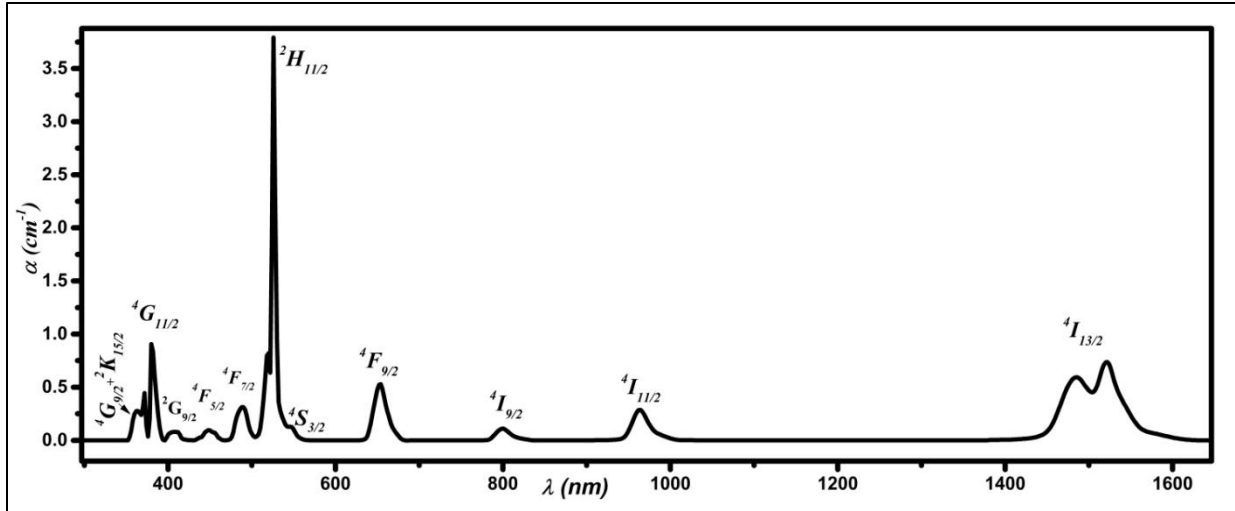


Fig.4. The absorption Coefficient spectra of PANBK1.5Er glass.

The electrostatic $F_{(2)}$, $F_{(4)}$, $F_{(6)}$ and spin-orbit (ζ) parameters were obtained using standard least-square fitting approach between calculated barycenter energies and experimental barycenter energies using RELEC program [RELIC 2013]. The calculations were made for PANBK1.5Er and the results are shown in Table.3 as a representative data .

Table.3. $F_{(2)}$, $F_{(4)}$, $F_{(6)}$ and ζ parameters for PANBK1.5Er

| | |
|-----------|---------------|
| $F_{(2)}$ | 431.3 |
| $F_{(4)}$ | 66.7 |
| $F_{(6)}$ | 7.3 |
| Z | 2436.5 |

The experimental oscillator strengths (f_{exp}) for all the absorption bands of Er^{3+} ions can be determined from the absorption spectra using the expression given by (equation 4) [Judd 1962].

$$f_{exp}(\Psi J \rightarrow \Psi' J') = \frac{mc^2}{\pi e^2} \int \epsilon(\nu) d\nu = 4.318 \times 10^{-9} \int \epsilon(\nu) d\nu \quad (4)$$

where m and e are the mass and the charge of the electron, respectively, c is the speed of light and ν is the wavenumber (cm^{-1}).

According to Jude-Ofelt theory [Judd 1962, Ofelt 1962] the total oscillator strength can be calculated using equation (5)

$$f_{calc}(\Psi J \rightarrow \Psi' J') = \frac{8\pi^2 m \nu_0}{3h(2j + 1)n^2} [\chi_{ed} S_{ed} + \chi_{md} S_{md}] \quad (5)$$

Where S_{ed} and S_{md} the electric and magnetic dipole strengths, $\chi_{ed} = n(n^2 + 2)^2/9$ and $\chi_{md} = n^3$ are the Dexter correction for the local field in a medium of refractive index n

$$S_{ed}(\Psi J \rightarrow \Psi' J') = \frac{8\pi^2 m \nu_0 \chi_{ed}}{3h(2j+1)n^2} \left[\sum_{t=2,4,6} \Omega_t |\langle i || U^t || j \rangle|^2 \right] \quad (6)$$

$$S_{md}(\Psi J \rightarrow \Psi' J') = \frac{e^2 h^2 \chi_{md}}{16\pi^2 m^2 c^2} |\langle i || L + 2S || j \rangle|^2 \quad (7)$$

Where Ω_t (t=2, 4, and 6) are Judd-Ofelt intensity parameters, m is the electron mass, ν_0 is the wavenumber at the maximum absorption (cm^{-1}), $2J+1$ is the degeneracy of the originating level of the transition, h is the Plank constant = 6.6261×10^{-27} erg.sec, and $\langle i || U^t || j \rangle$ are the doubly reduced matrix elements of the *tensor transition operator* and they have been calculated as in [Mohan 2007, P.Hehlen 2013] using [RELIC 2013].

The intensity parameters, Ω_t (t=2, 4, and 6) can be determined using least-square fitting approach between calculated (f_{calc}) and experimental (f_{exp}) oscillator strength.

The J.O parameters are sensitive to the glass composition. The value of Ω_2 is pointing to covalent bonding between surrounding ligands and rare earth ions, whereas Ω_4 and Ω_6 parameters are related to the rigidity of the medium [Jorgensen and Reisfeld 1983]. The Ω_t parameters of PANBK1.5Er glass compared to other reported data are tabulated in Table.4. It can be seen that the Ω_t parameters of the prepared glass is smaller than the other glasses which indicates that lower rigidity of the medium, lower covalency of the Er–O bond and asymmetry around Er^{3+} site. The spectroscopic quality factor ($\chi = \Omega_4/\Omega_6$) is important in predicting the lasing transitions in a given matrix [Qiao 2004]. The value of χ for the PANBK1.5Er glass has been calculated to be 0.795 and compared with those of the reported Er^{3+} glasses in Table.4. The value of χ for the present glass is larger than Phosphate [Babu 2007] but smaller than Sodium phosphate [Reddy 2011], Fluoride phosphate [Linganna 2015] and Antimony–borate [Qian 2010] glass, Lead phosphate [C.C.Santos 2009], Silicate [Qian 2008] glass and CaSc_2O_4 [Georgescu 2018] glass.

Table.4. The Judd–Ofelt parameters ($\Omega_t \times 10^{-20} \text{ cm}^2$), trend and spectroscopic quality factor ($\chi = \Omega_4/\Omega_6$) for PANBK1.5Er glass with other reported Er^{3+} -doped systems.

| HOST MATRIX | Ω_2 | Ω_4 | Ω_6 | $\chi = \Omega_4/\Omega_6$ | Trend |
|--|------------|------------|------------|----------------------------|----------------------------------|
| PANBK1.5Er | 0.43 | 0.31 | 0.39 | 0.795 | $\Omega_2 > \Omega_6 > \Omega_4$ |
| Present work | | | | | |
| Phosphate [Babu 2007] | 8.05 | 1.46 | 2.28 | 0.64 | $\Omega_2 > \Omega_6 > \Omega_4$ |
| Sodium phosphate [Reddy 2011] | 3.26 | 0.57 | 0.55 | 1.04 | $\Omega_2 > \Omega_4 > \Omega_6$ |
| Lead phosphate [C.C.Santos 2009] | 12.50 | 4.00 | 3.00 | 1.33 | $\Omega_2 > \Omega_4 > \Omega_6$ |
| Fluoride phosphate | 4.70 | 1.60 | 1.60 | 1.00 | $\Omega_2 > \Omega_4 = \Omega_6$ |

| [Linganna 2015] | | | | | |
|---|------|------|------|------|----------------------------------|
| Silicate [Qian 2008] | 4.20 | 1.85 | 1.62 | 1.14 | $\Omega_2 > \Omega_4 > \Omega_6$ |
| Antimony–borate [Qian 2010] | 2.63 | 1.04 | 1.09 | 0.95 | $\Omega_2 > \Omega_6 > \Omega_4$ |
| CaSc ₂ O ₄ [Georgescu 2018] | 3.42 | 1.66 | 0.76 | 2.18 | $\Omega_2 > \Omega_4 > \Omega_6$ |

Table 5 shows the experimental peak position ($E_{exp} \text{ cm}^{-1}$), calculated peak position ($E_{calc} \text{ cm}^{-1}$), experimental oscillator strengths ($f_{exp} \times 10^{-6}$), calculated oscillator strengths ($f_{calc} \times 10^{-6}$) and Judd-Ofelt intensity parameters for different transitions of Er³⁺ ions in PANBK1.5Er glass. The good agreement between experimental and calculated parameters indicates the accurate fitting of Judd-Ofelt parameters and electrostatic parameters.

Table 5. The E_{exp} , E_{calc} , f_{exp} , f_{calc} and Judd-Ofelt intensity parameters for different transitions of Er³⁺ ions in PANBK1.5Er glass.

| Initial level | Final level | Energy (cm^{-1}) | | $F \times 10^{-6}$ | |
|------------------------|------------------------|-----------------------------|------------|--------------------|------------|
| | | E_{exp} | E_{calc} | f_{exp} | F_{calc} |
| $^4I_{15/2}$ | $^4I_{13/2}$ | 6639.8 | 6676.8 | 0.66 | 0.93 |
| $^4I_{15/2}$ | $^4I_{11/2}$ | 10345.2 | 10303.5 | 0.23 | 0.18 |
| $^4I_{15/2}$ | $^4I_{9/2}$ | 12497.9 | 13364 | 0.09 | 0.09 |
| $^4I_{15/2}$ | $^4F_{9/2}$ | 15281.9 | 15213.2 | 0.7 | 0.52 |
| $^4I_{15/2}$ | $^4S_{3/2}$ | 18153.5 | 18280.1 | 0.2 | 0.16 |
| $^4I_{15/2}$ | $^2H_{11/2}$ | 19080.7 | 19218.7 | 2.7 | 0.96 |
| $^4I_{15/2}$ | $^4F_{7/2}$ | 20496.1 | 20381.9 | 0.57 | 0.61 |
| $^4I_{15/2}$ | $^4F_{5/2}$ | 22268.9 | 22019.1 | 0.25 | 0.2 |
| $^4I_{15/2}$ | $^2G_{9/2}$ | 24574.8 | 24583.3 | 0.19 | 0.24 |
| $^4I_{15/2}$ | $^4G_{11/2}$ | 26121.6 | 26513.4 | 1.29 | 1.55 |
| Ω_2 | Ω_4 | Ω_6 | | | |
| 0.43×10^{-20} | 0.31×10^{-20} | 0.39×10^{-20} | | | |

Once the Jude-Ofelt parameters have been obtained, some important radiative parameters can be derived such as :-

The spontaneous emission probability (A) of an electric-dipole transition is given by the following equation[Weber 1967].

$$A_r(\Psi J \rightarrow \Psi' J') = \frac{64\pi^4 \nu_0^2 e^2}{3h(2j+1)} \left[\frac{n(n^2+1)^2}{9} S_{ed} + n^3 S_{md} \right] \quad (8)$$

Where S_{ed} and S_{md} are the electric and magnetic dipole line strengths respectively which are expressed as

$$S_{ed}(\Psi J \rightarrow \Psi' J') = \sum_{t=2,4,6} \Omega_t | \langle J || U^t || J' \rangle |^2 \quad (9)$$

$$S_{md}(\Psi J \rightarrow \Psi' J') = \frac{h^2}{16\pi^2 m^2 c^2} | \langle J || L + 2S || J' \rangle |^2 \quad (10)$$

The total radiative transition probability $A_t(\Psi J)$ for an excited level is given by the sum of the $A(\Psi J \rightarrow \Psi' J')$ terms calculated over all terminal levels [Weber 1967].

$$A_t(\Psi J) = \sum A(\Psi J \rightarrow \Psi' J') \quad (11)$$

The fluorescence branching ratio B_r has been determined using

$$B_r = \frac{A(\Psi J \rightarrow \Psi' J')}{A_t(\Psi J)} \quad (12)$$

The radiative lifetime $\tau_r(\Psi J)$ of an excited level (ΨJ) is given by the reciprocal of $A_t(\Psi J)$ [Weber 1967].

$$\tau_r(\Psi J) = \frac{1}{A_t(\Psi J)} \quad (13)$$

The A , τ_r and β_r for the emission levels of Er^{3+} ions for PANBK1.5Er glass, are presented in

Table.6. The τ_r for the ${}^4I_{13/2} \rightarrow {}^4I_{15/2}$ transition is about 11.53ms. It can be observed that the τ_r for the present glass is much higher than, calcium barium phosphate glasses [Luewarasirikul 2018] ($\tau_r = 2.7$ ms), lead phosphate ($\tau_r = 3.7$ ms) [C.C.Santos 2009], silicate ($\tau_r = 3.82$ ms) [Qian 2008], phosphate ($\tau_r = 4.82$ ms) [Babu 2007] and sodium phosphate ($\tau_r = 10.57$ ms)[Reddy 2011]. Hence, the prepared phosphate glasses can be considered very promising to active laser application. The same thing for the green line emission at 543nm for the ${}^4S_{3/2} \rightarrow {}^4I_{15/2}$ transition, it have high radiative lifetime ($\tau_r = 1.749$ ms) and high branching ratio ($\beta_R = 0.67212$).

Table.6. A_{rad} , τ_r and β_r for the ${}^4S_{3/2} \rightarrow {}^4I_{15/2}$ and ${}^4I_{13/2} \rightarrow {}^4I_{15/2}$ transitions of Er^{+3} ions in PANBK1.5Er glass.

| INITIAL LEVEL | FINAL LEVEL | τ_{rad} | A_{rad} | Branching Ratio (B_r) |
|----------------|----------------|--------------|--------------|---------------------------|
| ${}^4S_{3/2}$ | ${}^4F_{9/2}$ | | 0.32 | 0.0006 |
| ${}^4S_{3/2}$ | ${}^4I_{9/2}$ | | 18.59 | 0.0325 |
| ${}^4S_{3/2}$ | ${}^4I_{11/2}$ | 1.749 | 10.96 | 0.01917 |
| ${}^4S_{3/2}$ | ${}^4I_{13/2}$ | | 156.14 | 0.27302 |
| ${}^4S_{3/2}$ | ${}^4I_{15/2}$ | | 385.89 | 0.67475 |
| ${}^4I_{13/2}$ | ${}^4I_{15/2}$ | 11.53 | 86.73 | 1 |

McCumber equation [McCumber 1964] relates absorption and emission cross-section as follows :-

$$\sigma_e(\nu) = \sigma_a(\nu)e^{(\varepsilon-h\nu)/K_B T} \quad (14)$$

Where ε is as the net free energy required to excite one Er^{3+} ion from the ${}^4I_{15/2}$ to the ${}^4I_{13/2}$ state at temperature T . The absorption cross-section (σ_a) has been calculated by equation (15) [Miniscalco and Quimby 1991].

$$\sigma_a = 2.302 \frac{A}{NL} \quad (15)$$

where A is the absorbance , N is the Er^{+3} ion concentration per cubic cm and L is the sample thickness.

The absorption (σ_a) and emission (σ_e) cross-sections of Er^{3+} ions ${}^4I_{13/2} \rightarrow {}^4I_{15/2}$ transition in PANBK1.5Er glass are presented in Fig.5. From this figure it is clear that the peaks of absorption and emission cross-sections of Er^{+3} are 1522 nm (λ_p). At longer wavelengths σ_e is higher than σ_a , and for shorter wavelengths σ_e is smaller than σ_a .

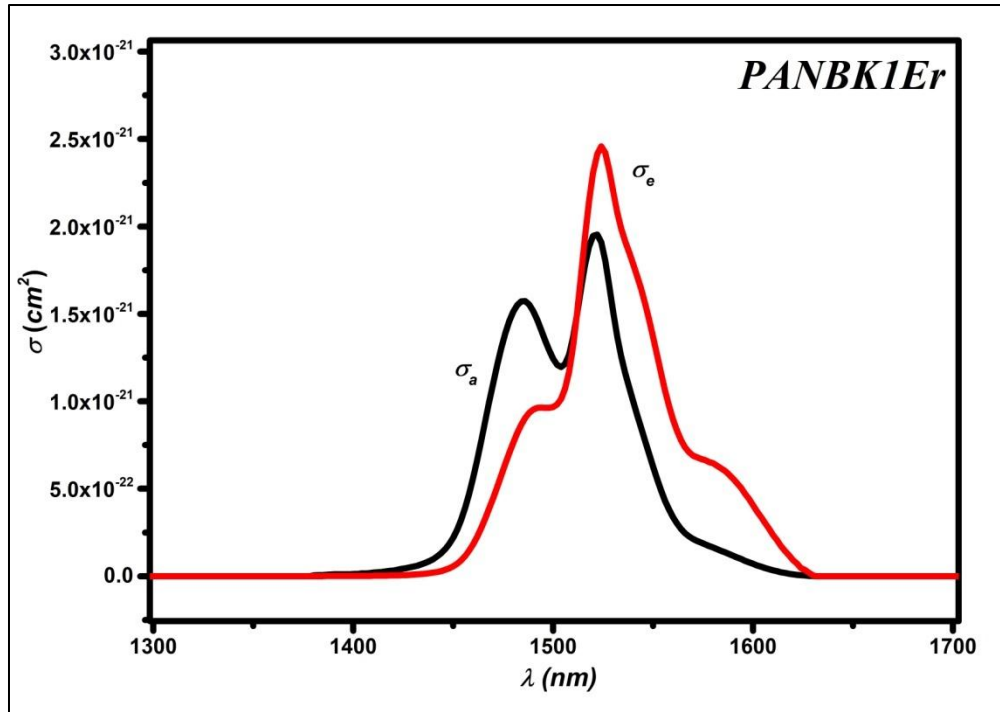


Fig.5.The absorption (σ_a) and emission (σ_e) cross-sections of $4I13/2 \rightarrow 4I15/2$ transition vs wavelength in PANBK1.5Er.

The internal gain coefficient (G) as a function of wavelength λ can be estimated by means of the formula

$$G(\lambda) = \sigma_e(\lambda)N_2 - \sigma_a(\lambda)N_1 \quad (16)$$

Where N_1 and N_2 are the concentration of ions in the ground and excited state, respectively and $N_1+N_2 = N$ where N is being the total concentration of erbium ions in the sample) [E.Desurvire 1994]. The population inversion rate is given by

$$P = \frac{N_2}{N} \quad (17)$$

Fig.6 displays internal gain coefficient spectra as a function of inverted population rate. From this spectrum, it is observed that lasing would be achieved around 1596 nm with only 20% Population inversion ($P = 0.2$). A gain of 0.1 dB.cm^{-1} and nearly a flat band width are obtained. When increasing P , the gain's peak shifts to the shorter wavelength. For complete population inversion ($P=1$) the peak centered at 1522 nm, the effective bandwidth = 64.8 nm and the gain is equal to 9.67 dB cm^{-1} .

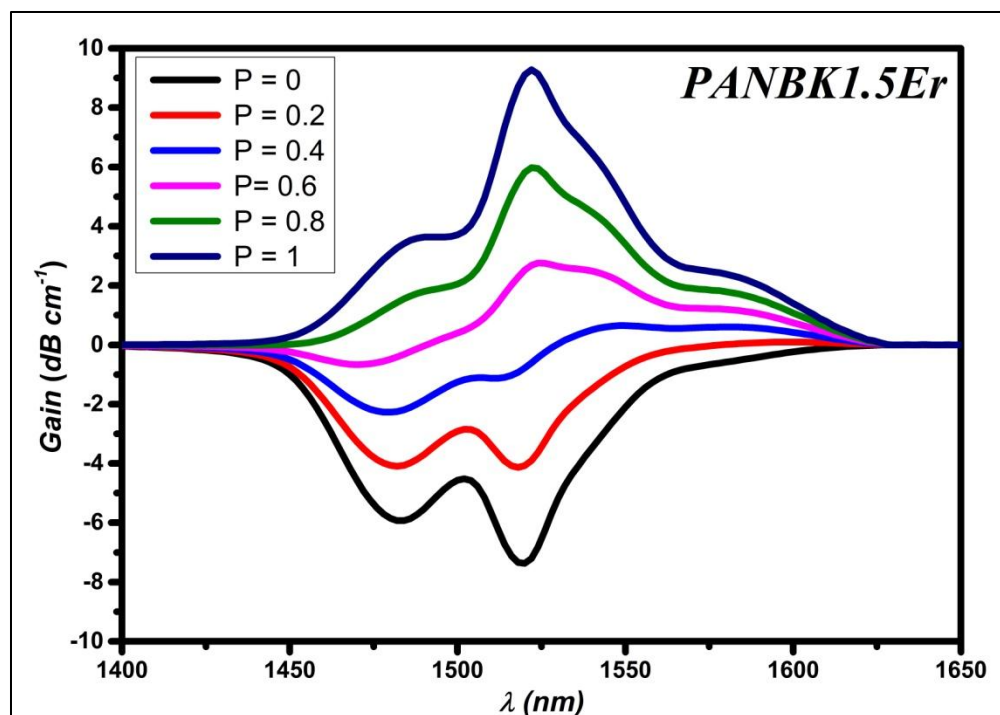


Fig.6. The gain spectra as a function of inverted population rate ($P = 0, 0.2, 0.4, 0.6, 0.8$ and 1) in PANBK1.5Er glass.

4 Conclusion

Er^{3+} doped Na-Al-Ba-K phosphate glasses have been prepared by melt quenching technique. Absorption spectra have been analyzed using the Judd-Ofelt theory. The Judd-Ofelt parameters of the present glass is smaller than other compared glasses which indicates that lower rigidity of the medium, lower covalency of the Er-O bond and asymmetry around Er^{3+} site. Higher radiative lifetime for the ${}^4I_{13/2}$ level of Er^{3+} ions has been noticed compared to the other Er^{3+} doped glasses. The emission cross-section has been evaluated using Mc-Cumber theory hence the gain cross-section has been evaluated as a function of population inversion, which clarify that the amplification action achieved at $1.522 \mu\text{m}$. These results obviously indicate that present glasses are suitable for laser as well as optical amplifiers around 543 nm and $1.522 \mu\text{m}$ regions.

References

- A. A. Reddy, S. S. Babu, K. Pradeesh, C. J. Otton and G. V. Prakash, Optical properties of highly Er³⁺-doped sodium–aluminium–phosphate glasses for broadband 1.5 μm emission, *J. Alloy. Compd.* 509((2011) 4047-4052.
- A. Lira, C. I. Camarillo, E. Camarillo, F. Ramos, M. Flores, U. Caldino, Spectroscopic characterization of Er³⁺ transitions in Bi₄Si₃O₁₂, *J. Phys.: Condens. Matter.* 16 (2004) 5925-5936.
- A. M. Y. Ohishi, M. Yamada, H. Ono, Y. Nishida, K. Oikawa, Gain characteristics of tellurite-based erbium-doped fiber amplifiers for 1.5-μm broadband amplification, *Opt. Lett.* 23(1998) 274-276.
- B. R. Judd, Optical absorption intensities of rare earth ions, *Phys. Rev.* 127(1962) 750.
- C.C.Santos, I.Guedes, C.K.Loong, L.A.Boatner, A.L.Moura, M. T. d. Araujo, C.Jacinto and M.V.D.Vermelho, Spectroscopic properties of Er³⁺-doped lead phosphate glasses for photonic application, *Physics D: Applied Physics.* 43(2) (2009) 025102. Doi:10.1088/0022-3727/43/2/025102
- C. K. Jorgensen and R. Reisfeld, Judd–Ofelt parameters and chemical bonding, *Less-Common Met.* 93 (1983) 107.
- D. E. McCumber, *Phys. Rev.* 134(1964) A299-A306.
- E.Desurvire (1994). *Erbium-Doped Fiber Amplifiers, Principles and Applications.* New York, John Wiley.
- G. S. Ofelt, Intensities of Crystal Spectra of Rare-Earth Ions, *Chemical Physics.* 37(1962) 511-520. Doi:10.1063/1.1701366.
- K. Linganna, K. Suresh, S. Ju, W. T. Han, C. K. Jayasankar and V. Venkatramu, Optical properties of Er³⁺-doped K-Ca-Al fluorophosphate glasses for optical amplification at 1.53 μm, *OPTICAL MATERIALS EXPRESS.* 5(8) (2015) 1689-1703. DOI:10.1364/OME.5.001689
- M. J. Digonett (2001). *Rare-Earth-Doped Fiber Laser and Amplifier*, Marcel Dekker, Inc.
- M. P.Hehlen, MikhailG.Brik and KarlW.Krämer, 50th anniversary of the Judd–Ofelt theory: An experimentalist’s view of the formalism and its application, *Journal of Luminescence.* 5136(2013) 221-239. Doi:10.1016/j.jlumin.2012.10.035.
- M. Yamada, H. Ono, T. Kanamori and Y. Ohishi. , Broadband and gain flattened amplifier composed of a 1.55 μm-band and 1.58 μm-band Er³⁺ - doped fiber amplifier in a parallel configuration *Electron Lett.* 33(1997) 710-711.
- M.Yamane and Y.Asahara (2004). *Glasses for Photonics*, Cambridge University Press.
- N. Luewarasirikul, N. Chanthima, Y. Tariwong and J. Kaewkhao, Erbium-doped calcium barium phosphate glasses for 1.54 μm broadband optical amplifier, *Materials Today: Proceedings.* 5(6, Part 1) (2018) 14009-14016. Doi:10.1016/j.matpr.2018.02.053
- P. Babu, H. J. Seo, K. H. Jang, R. Balakrishnaiah, C. K. Jayasankar, K.S. Lim and V. Lavín, 1.5 μm emission, and upconversion properties of Er³⁺-doped metaphosphate laser glasses, *J. Opt. Soc. Am. B.* 24 (2007) 2218-2228.

Q. Qian, Q. Y. Zhang, H. F. Jiang, Z. M. Yang and Z. H. Jiang, The spectroscopic properties of Er^{3+} -doped antimony–borate glasses, *Physica B*. 405(2010) 2220-2225.

Q. Qian, Y. Wang, Q. Y. Zhang, G. F. Yang, Z. M. Yang and Z. H. Jiang, Spectroscopic properties of Er^{3+} -doped $\text{Na}_2\text{O-Sb}_2\text{O}_3\text{-B}_2\text{O}_3\text{-SiO}_2$ glasses, *Non-Cryst. Solids*. 354(2008) 1981-1985.

RELIC (2013). <https://www.lanl.gov/projects/feynman-center/deploying-innovation/intellectual-property/software-tools/relic/index.php>.

S. Georgescu, A. Ștefan and O. Toma, Judd-Ofelt analysis of Er-doped CaSc_2O_4 revisited, *Journal of Luminescence*. 199 (2018) 488-491. Doi:10.1016/j.jlumin.2018.03.086

S. Mohan, K. S. Thindb and G. Sharmab, Effect of Nd^{3+} Concentration on the Physical and Absorption Properties of Sodium-Lead-Borate Glasses, *Brazilian Journal of Physics*. 37(4) (2007) 1306-1313. Doi:10.1590/S0103-97332007000800019

W. J. Miniscalco and R. S. Quimby, General procedure for the analysis of Er^{3+} cross sections, *Optics Letters*. 16(1991) 258-260.

X. Qiao, X. Fan, M. Wang and X. Zhang, Up-conversion luminescence and near infrared luminescence of Er^{3+} in transparent oxyfluoride glassceramics, *Opt. Mater*. 27((2004) 597-603.

M. J. Weber, Probabilities for Radiative and Nonradiative Decay of Er^{3+} in LaF_3 , *PHYSICAL REVIEW*. 157(2) (1967) 262-272. DOI: 10.1103/PhysRev.157.262

الملخص باللغة العربية

الخواص الضوئية لزجاج الفوسفات المطعم بالاربيوم

محمود محمد اسماعيل^١، حازم فاروق^٢، محمد على سالم^١، عادل عشيري^١، ايناس كمال بطيشه^١

^١قسم فيزياء الجوامد، شعبة البحوث الفيزيائية، المركز القومي للبحوث، القاهرة، مصر

^٢قسم الفيزياء، كلية العلوم، جامعة الأزهر، القاهرة، مصر

تم تحضير زجاج الفوسفات المطعم بأيونات الاربيوم باستخدام طريقة الصهر والتبريد المحكوم. تم قياس طيف الامتصاص ومنه تم حساب معامل الامتصاص ومساحة مقطع الامتصاص للعينات. تم حساب مساحة مقطع الانبعاث باستخدام نموذج ماك كيمبر. تم تعيين الكسب كدالة في معدل الانقلاب التسكيني والذي بين امكانية التكبير حول الطول الموجي ١٥٩٦ نانو متر عند معدل انقلاب تسكيني ٢٠% فقط. تم استخدام نموذج جود اوفلت ومن ثم تم تعيين الخواص الاشعاعية للانتقالات $^4I_{15/2} \rightarrow ^4S_{3/2}$ و $^4I_{13/2} \rightarrow ^4I_{13/2}$. لوحظ ان فترة عمر المستوى $^4I_{13/2}$ للزجاج المحضر هي اكبر من مثيلاتها في تركيبات اخرى. تشير كل النتائج الى ان الزجاج المحضر مناسب وواعد لتطبيقات الليزر وعملية التكبير الضوئي حول الاطوال الموجية ٤٤٣ نانومتر و ١٥٢٢ نانومتر.